METALLOGRAPHIC AND MAGNETIC PROPERTIES
OF ALLAN HILLS 762 IRON METEORITE

R. M. FISHER, C. E. SPANGLER, Jr.,

U.S. Steel Corp., Research Laboratory, Monroeville, Pennsylvania 15146, U.S.A.

Takesi NAGATA and Minoru FUNAKI

National Institute of Polar Research, Kaga 1-chome, Itabashi-ku, Tokyo 173

Abstract: Allan Hills 762 a 1.5 kg iron meteorite from West Antarctica, contains 7.2 % Ni, 0.6 % Co, and 0.4 % P, and is identified as a very coarse octahedrite from its chemical and metallographic properties. According to WASSON, its genetic classification is group IAB, similar to Neptune Mountain also found in the Antarctic. Magnetic and metallographic analyses revealed that the structure is primarily well-annealed kamacite of 6.4 % Ni with a small amount of comb plessite, grain boundary schreibersite, and numerous rhabdite particles.

Two very unusual microstructural features were observed. Many of the narrow taenite bands contain small pools of kamacite in what may be termed a very coarse plessite structure which apparently formed during prolonged heating at moderate temperatures of about 450°C. All phosphide, $(FeNi)_3P$, particles are surrounded by a narrow ragged rim of taenite. A possible mechanism for the occurrence of those previously unobserved structures is proposed.

1. Introduction

The details of the discovery of a large number of stony, and a more limited number of iron meteorites in several areas in Antarctica have been described in detail in previous Proceedings of this series of symposia, as well as in other papers in this particular volume. In brief, nearly a thousand meteorite pieces were found on an area now called the Meteorite Ice Field located near the Yamato Mountains during four seasons of Japanese field explorations. These findings included 2 irons, 1 stony iron, 5 carbonaceous chondrites, with the remainder mostly ordinary chondrites and a few achondrites (NAGATA, 1975; NAGATA *et al.*, 1976; YANAI, 1975).

The differential mass distribution spectrum of these pieces is in agreement with that expected from the fragmentation model for small asteroidal bodies and it is clear that numerous meteorite showers are responsible for the findings (NAGATA,

1978).

Subsequently, more than 320 pieces were found in very similar ice fields near the Transantarctic Mountains in West Antarctica by U.S.-Japan joint teams during the field seasons 1976–77 and 1977–78 (CASSIDY et al., 1977).

The mechanism of the concentration of meteorites in particular positions in blue ice fields has been analyzed in detail (NAGATA, 1978). In summary, meteorites that have fallen up to 10^5 years ago are transported at a velocity of several meters/ year by ice sheet movements which result in a horizontal convergence and upwell of ice flow because of the underlying bedrock topography. Rapid ablation (up to 6 cm/year—comparable to the upwell velocity) removes the accumulation of snow cover and exposes the meteorites in these favorable locations.

The metallographic and magnetic properties of the 2 Yamato irons and the stony iron have been described previously (NAGATA et al., 1976; FISHER et al., 1978). In this paper we discuss the magnetic and metallographic properties of the single iron meteorite designated Allan Hills 762 found in January 1977.

2. General Description of Allan Hills 762 Meteorite

Allan Hills 762 iron meteorite is irregularly shaped with maximum dimensions through the different cross-sections of about 8 cm. The weight of the piece as found is 1510 grams with an apparent density of 7.812. The surface of the sample, black in color, is typical of the fusion crust on iron meteorites. A color photograph of Allan Hills 762 lying in place on blue ice can be seen in Fig. 12 of YANAI paper (1978). There is almost no evidence of extensive internal melting in contrast to the smaller Yamato iron sample examined previously. In cross-section, the depth of the reheated zone ranges from 2 to 4 mm, as can be seen in Fig. 1, and more clearly at higher magnification in some of the subsequent micrographs.

The very coarse octahedrite structure and vestigial traces of the kamacite
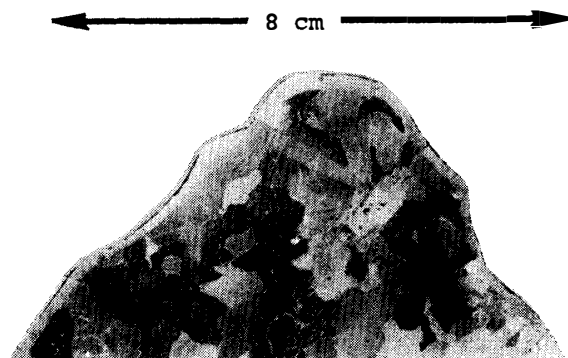
Fig. 1. Half cross-section of Allan Hills 762 iron meteorite showing coarse octahedrite grain structure, shallow ablation negmaglypts and the reheated rim.
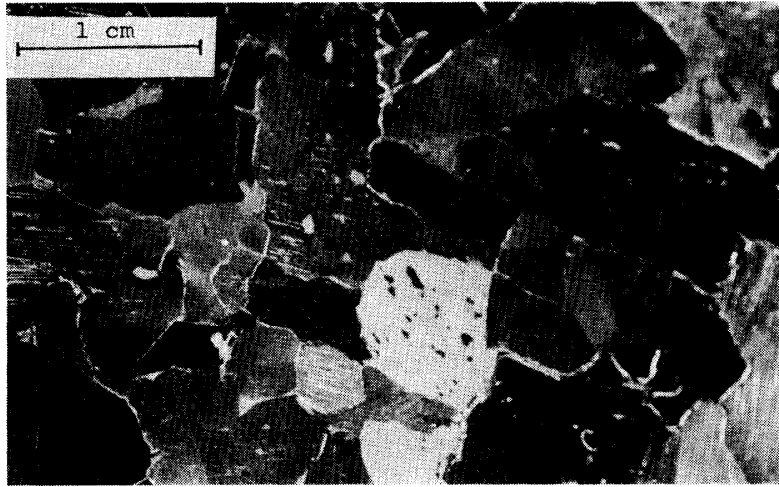
Fig. 2. Kamacite band width (3-4 mm) is more evident at higher magnification. Striations are from cutting.
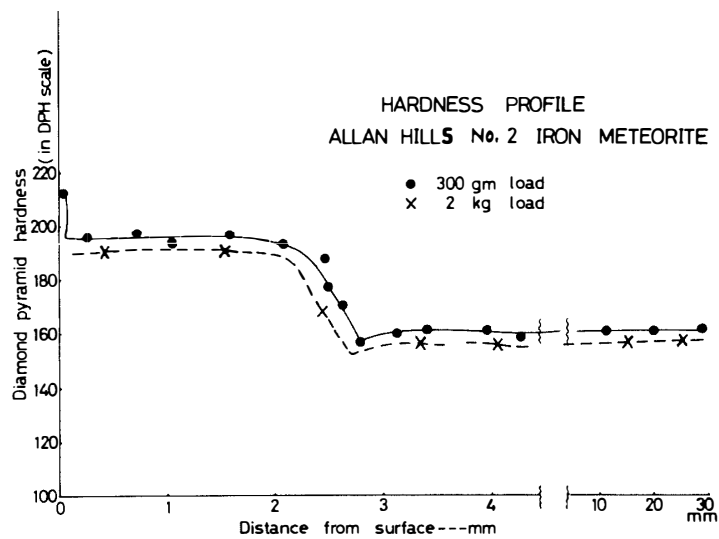
Fig. 3. Type III hardness profile showing α_2 rim and fully annealed interior.

bands are more evident at higher magnification in Fig. 2. The kamacite grains range from 2 to 5 mm in diameter.

The hardness varied across the cross-section, as shown plotted in Fig. 3. This hardness profile is typical of Type III as given by BUCHWALD (1975), and indicates that the meteorite was in almost a perfectly annealed state before it reached the earth's atmosphere. In addition to the hardness profile in this figure, the hardness of individual grains in other areas well within the interior of the sample was also determined to confirm that the level is maintained throughout the cross-section.

The results of qualitative X-ray fluorescence analysis of the coarse section of Allan Hills 762 iron meteorite and radiochemical data on small pieces (WASSON, 1978) are shown in Table 1.

Table 1. Chemical composition of two Antarctic iron meteorites.

Designation	Weight (gm)	Density (gm/cm³)	Ni	Co	P (wt/%)	Ga	Ge	Ir
Allan Hills 762 (Group IAB)	1510	7.812	7.2	0.6	0.4	~90	~400	~2*
Neptune Mountain (Group IAB)	1070	—	7.1	—	0.20	73.9	269	2.0**

* Preliminary estimates from John WASSON (1978).
** WASSON data quoted in BUCHWALD (1975).

The Ni and P contents and the very coarse grain structure of Allan Hills 762 suggest that it is a coarsest octahedrite of structure type 0_{gg}. This supposition is strongly supported by preliminary radiochemical data kindly supplied by John WASSON and which also places it in group IAB of the genetic classification system (SCOTT and WASSON, 1975).

3. Metallographic Examination

The appearance of the reheated zone surrounding Allan Hills 762 iron meteorite is seen clearly in Fig. 4. Narrow bands of taenite comprising comb plessite, small blebs of schreibersite in the kamacite grain boundaries and fine rhabdites are also visible.
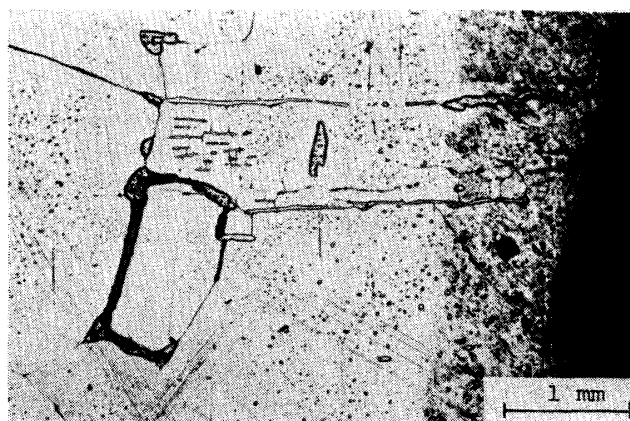
Fig. 4. Fine α_2 transformation structure in the reheated rim, comb plessite and schreibersite in the kamacite grain boundaries.
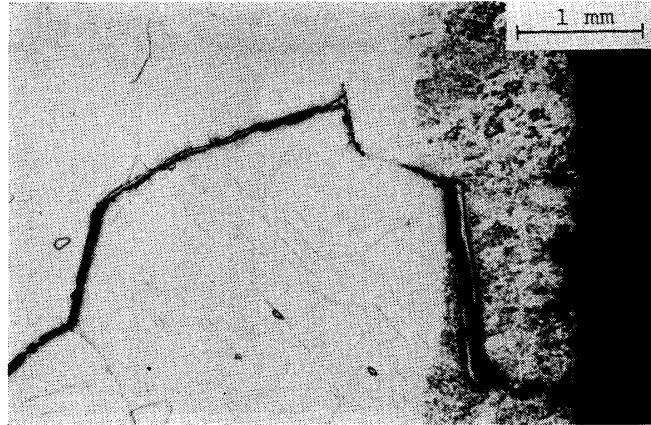
Fig. 5.   Incipient melting and penetration of oxide along schreibersite in kamacite grain boundaries.
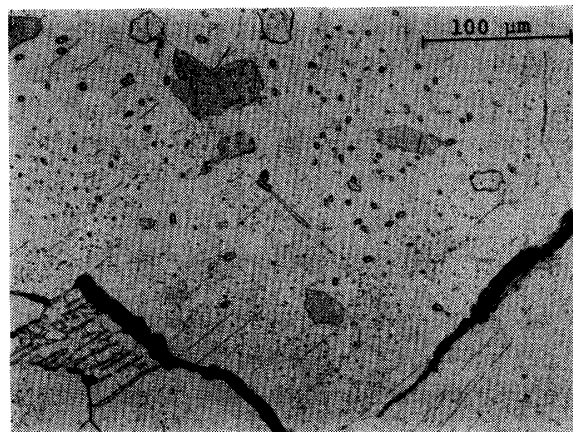
Fig. 6.   Oxide penetration along grain boundary of recrystallized schreibersite and comb plessite: kamacite and rhabdites are also seen.

In some regions, where schreibersite extended into the reheated zone, incipient melting and oxide penetration occurred along kamacite grain boundaries as seen in Fig. 5.   Sometimes this penetration extended up to 8 mm into the interior of the sample as shown in Fig. 6.   A scanning electron micrograph (SEM) of oxide penetrating through schreibersite is shown in Fig. 7.   A thin taenite rim to be discussed further below may also be seen.

The fine structure of the α_2 transformation due to reheating during passage through the earth's atmosphere is visible in the SEM and optical micrographs of an etched sample in Fig. 8.

A good example of comb plessite is shown at higher magnification in Fig. 9. Several small blebs of schreibersite and numerous fine rhabdites are also present. Regions A (top) and B are marked for further attention.   These are shown in
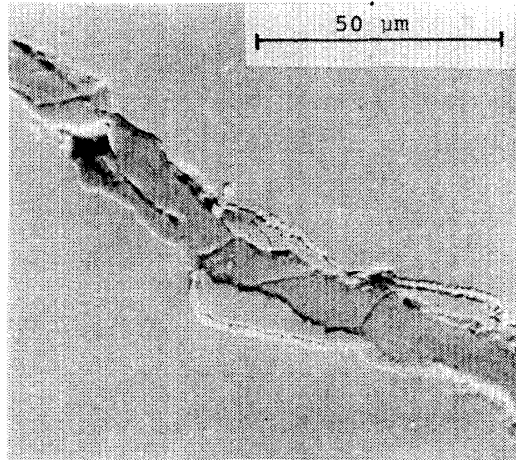
Fig. 7.   SEM of oxide penetration along schreibersite with thin taenite rim.
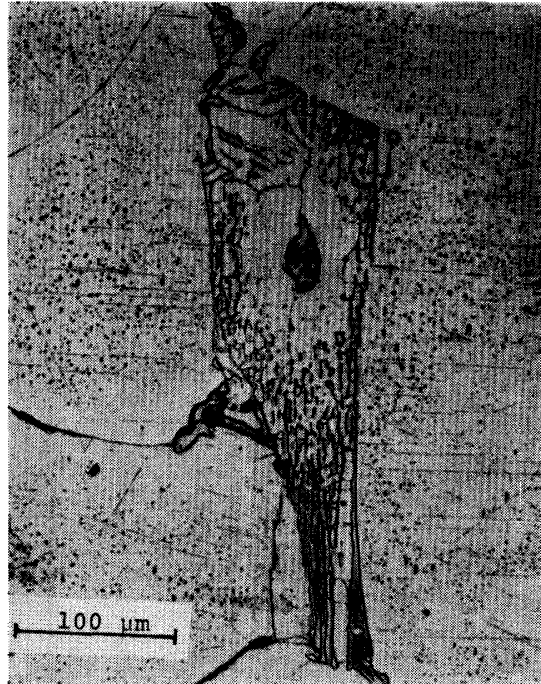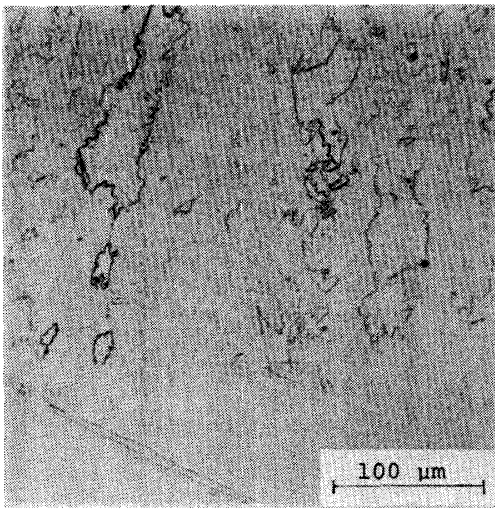
*Fig. 9.   Comb plessite surrounding schrei-
bersite blebs and numerous rhabdites
in the kamacite matrix.*
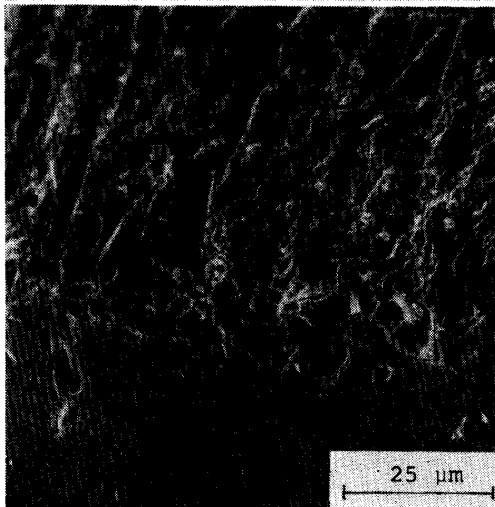
*Fig. 8.   Inside edge of α_2 reheated rim in
Allan Hills 762 iron meteorite. Top:
optical micrograph; Bottom: scanning
electron micrograph.*
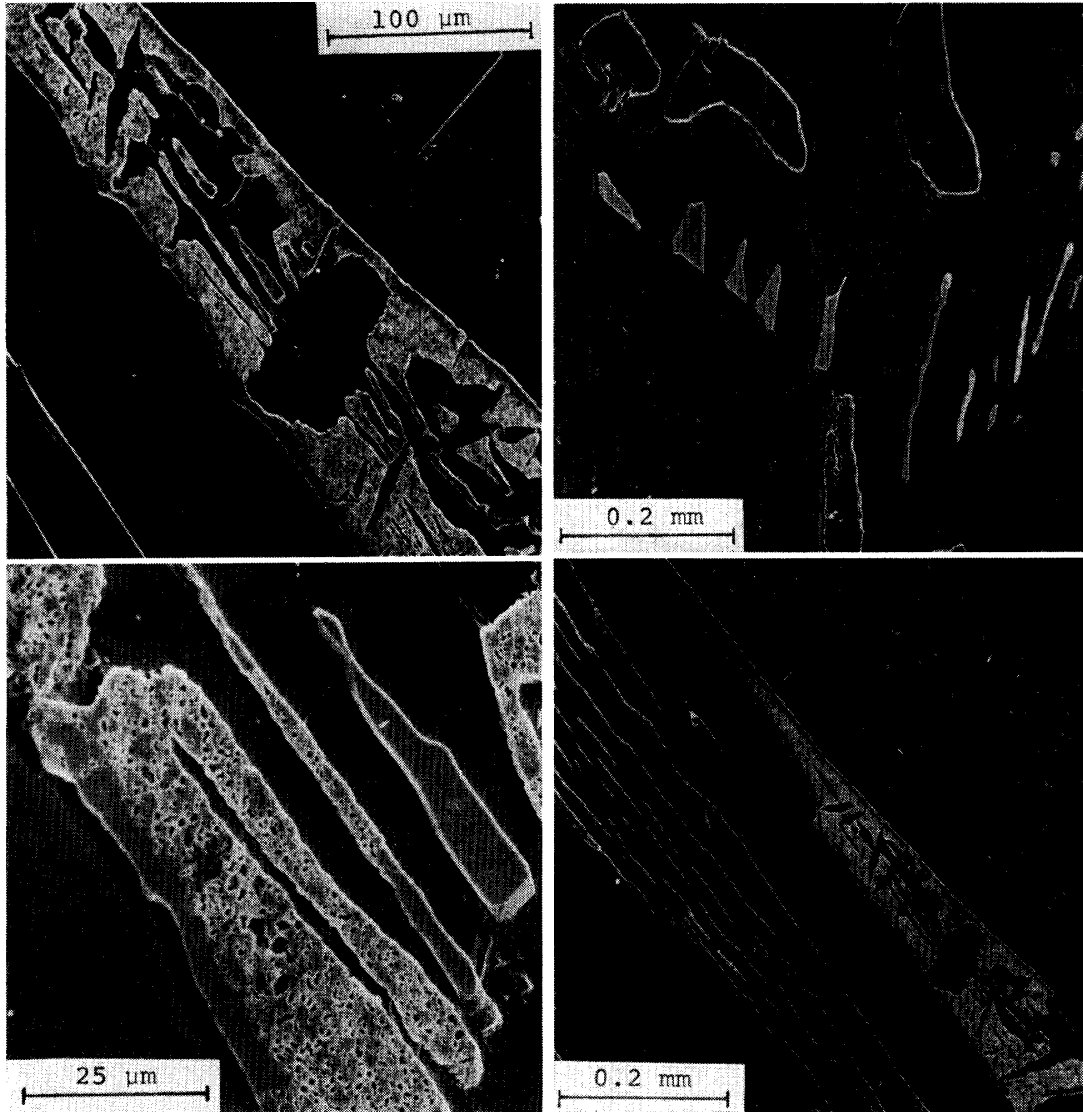
Fig. 10.   SEM of region A (top) and B (bottom) (slightly rotated clockwise) of comb plessite in Fig. 9.

Fig. 11.   Higher magnification (of Figs. 9 and 10) reveals fine structure in taenite in comb plessite.

scanning electron micrographs at high magnifications in Figs. 10 and 11. The clear area standing in relief above the kamacite matrix are high nickel taenite.

Fig. 12 shows the results of qualitative X-ray analysis of the unreacted taenite and the fine kamacite regions and the adjacent Ni-enriched taenite rim. This structure can be considered as a coarse plessite and presumably formed during prolonged heating around 500°C as discussed below.

An example of a schreibersite particle completely enclosed by taenite is shown

$k_\alpha k_\beta$ $k_\alpha k_\beta$
Fe   Ni
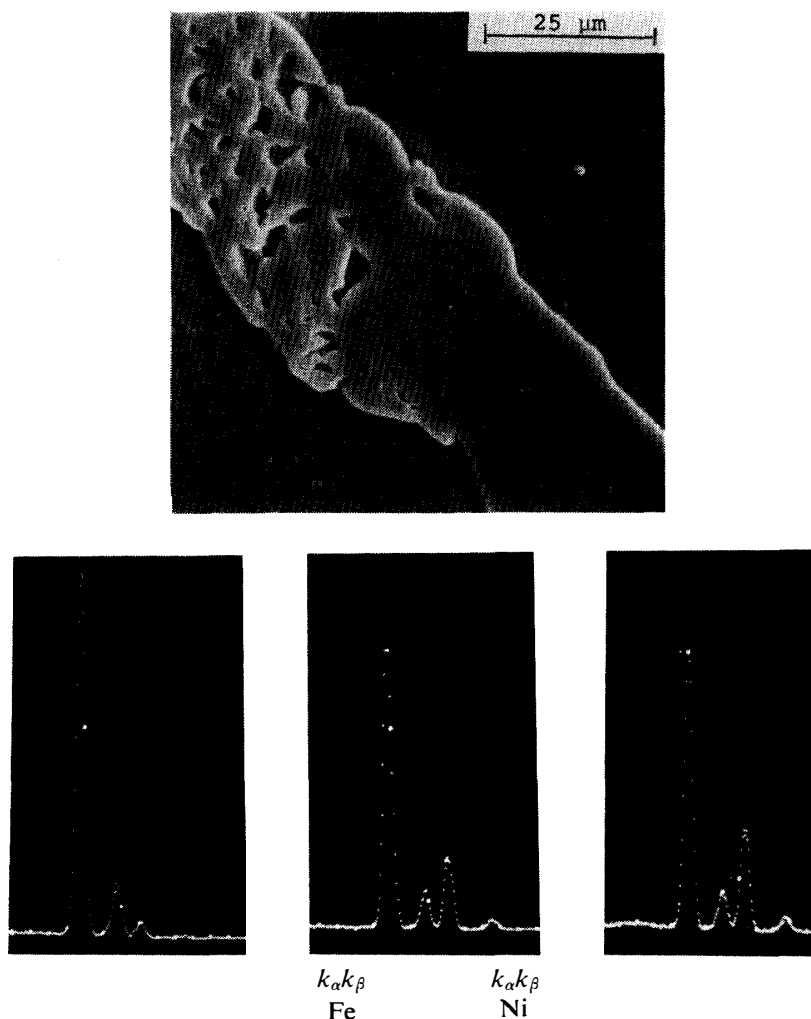
Fig. 12.   Qualitative X-ray analysis of taenite band shows ~30% Ni in unreacted zone in kamacite pools, and ~35% Ni adjacent to kamacite pools.

in the SEM in Fig. 13 (top).   More often the rim consists of disconnected taenite areas.   Examples of rhabdites encased by a decomposed taenite are shown in Fig. 14.   When the rhabdites are very small decomposition of the taenite does not always occur as shown in Fig. 15, which also includes results of qualitative X-ray analysis.   The phosphides are high in nickel, in keeping with their formation at a relatively low temperature.

Similar decomposed taenite is observed along schreibersite blebs although the structure tends to be much finer, as illustrated in Fig. 16.

4.   Magnetic Properties

Characteristics of the magnetic hysteresis curve of interior part (excluding
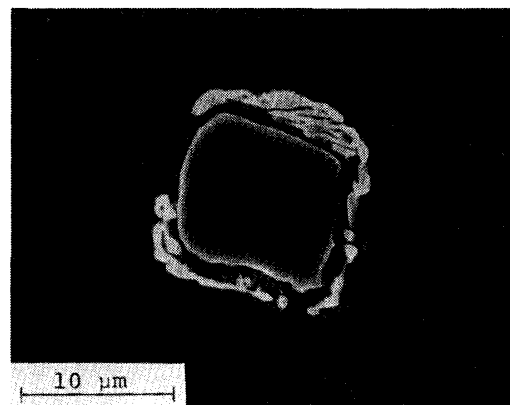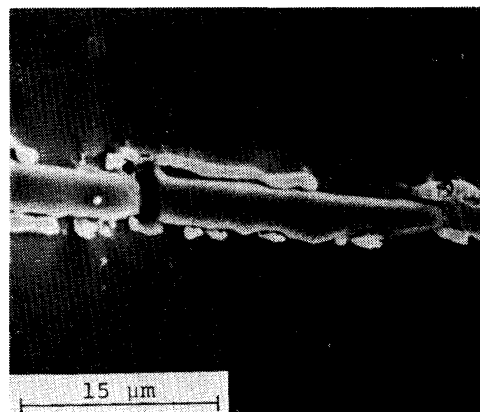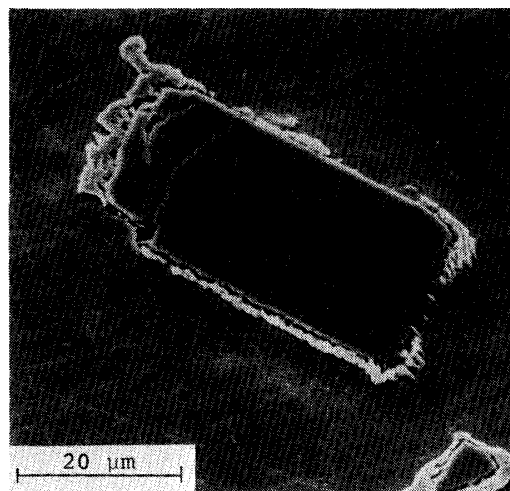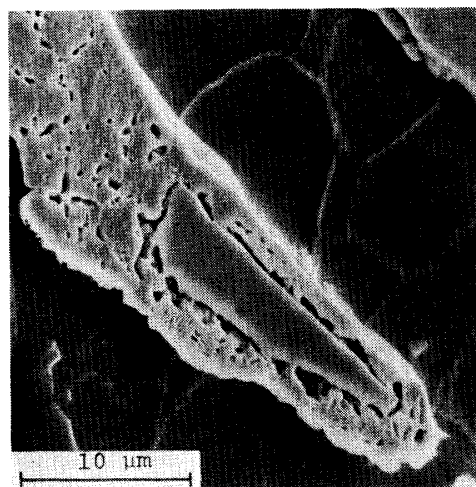
Fig. 13.   (Top) Small schreibersite crystal enclosed in decomposed taenite band. (Bottom) Vestigial taenite rim around iron-nickel phosphide particle.

Fig. 14.   Examples of rhabdites with decomposed taenite rim.

the fusion crust) of Allan Hills 762 at room temperature (20°C) are represented by

Magnetic susceptibility:	$\chi_0(20°C)$	$= 0.048$ emu/gm/Oe,
Saturation magnetization:	$I_s(20°C)$	$= 210$ emu/gm,
Saturation remanence:	$I_R(20°C)$	$= 0.3$ emu/gm,
Coercive force:	$H_c(20°C)$	$= 6.2$ Oersteds,
Remanence coercive force:	$H_{Rc}(20°C)$	$= 130$ Oersteds.

The thermomagnetic curve of the sample was repeatedly examined in a magnetic field of 950 Oe.   The first-run thermomagnetic curve is illustrated in Fig. 17 which is practically identical to the second-run thermomagnetic curve.   As shown in the figure, the $\alpha \to \gamma$ transition temperature in the heating process is given by $\Theta^*_{\alpha \to \gamma} = 770°C$ and the $\gamma \to \alpha$ transition temperature in the cooling process by $\Theta^*_{\gamma \to \alpha} = 639°C$,
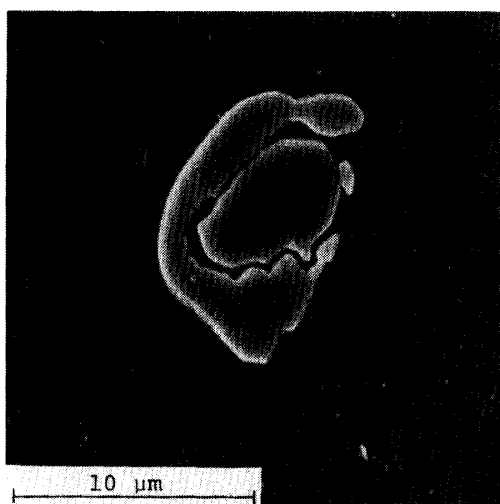
Fig. 15. Taenite rim around very small
Fe–Ni phosphide particle. FeNi₃P:~
65%Fe–20%Ni%15%P, Taenite rim:
~70%Fe–30%Ni, Kamacite: ~93.5
%Fe–6.5%Ni.
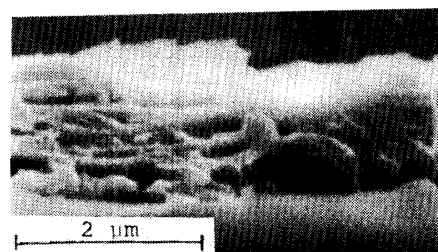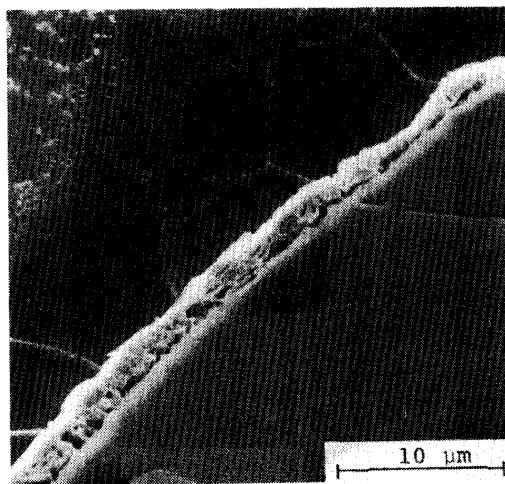
Fig. 16. Decomposed taenite rim around
schreibersite bleb.

which indicate that the average content of Ni in kamacite phase is 6.5 wt%. Fig. 17 suggests that this iron meteorite is composed mostly of a single metallic phase of 6.5 wt% Ni kamacite, which is chemically identified as a coarse octahedrite. The observed value of $I_s(20°C)$ also suggests that this iron meteorite consists almost entirely of either a hexahedrite or a Ni-poor octahedrite.

Although the intrinsic magnetic parameters such as I_s, $\Theta^*_{\alpha \to \gamma}$ and $\Theta^*_{\gamma \to \alpha}$ are stable and reproducible in laboratory-scale heat treatments up to about 800°C, suggesting that the major parts (i.e. the kamacite phase) of this iron meteorite are in a well annealed state, the structure sensitive magnetic parameters such as χ_0, I_R and H_c are reduced considerably by a heat treatment in vacuum (10^{-5} Torr air) up to 800°C. Namely, after such a heat treatment these parameters have become $\chi_0 = 0.029$ emu/ gm/Oe, $I_R = 0.05$ emu/gm and $H_c = 1.6$ Oe. The considerable decreases in I_R and H_c may be due to a release of internal mechanical stresses caused by the presence of minor constituents such as schreibersites and rhabdites.
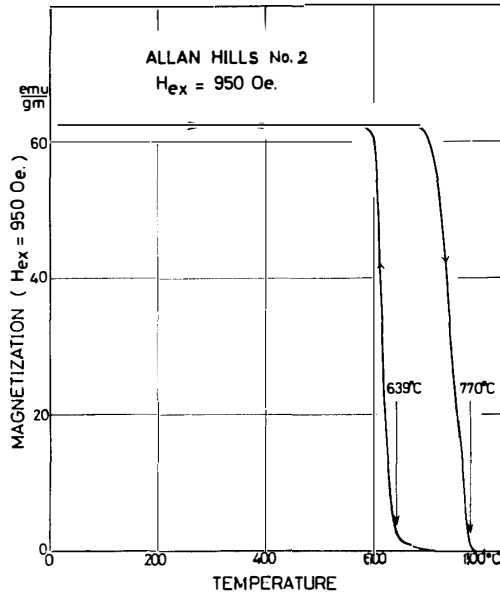
Fig. 17.   Thermomagnetic curve indicating average kamacite composition of 6.5% Ni.

5.   Summary and Discussion

Chemical, magnetic and metallographic analyses have shown that Allan Hills 762 is a very coarse octahedrite with 6.4% Ni kamacite as the major phase. Only small regions of comb plessite and relatively tiny schreibersite blebs and rhabdites remain as vestiges of the parent taenite.   According to the detailed studies
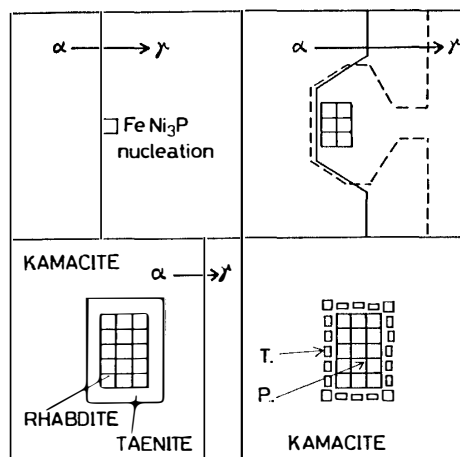
Fig. 18.   Schematic illustration of formation of Ni-rich taenite rim around rhabdites nucleated on transformation interface.   Decomposition of taenite may occur during subsequent cooling.

of GOLDSTEIN and DOAN (1972), equilibrium transformation to kamacite will commence around 760°C. In this relatively high P (0.4%) meteorite, precipitation of schreibersite along kamacite grain boundaries and rhabdites along the α/γ transformation interface will follow shortly after ~ 720°C.

An unusual feature observed in this meteorite, possibly for the first time, is the occurrence of a high nickel (30%Ni) rim around all phosphide particles. In most cases this taenite shows evidence of decomposition by a ragged intrusion of the adjacent kamacite. A possible mechanism for the origin of this structure is illustrated schematically in Fig. 18. It is generally beleived that nucleation of rhabdites occurs on the transformation interface and it has been assumed on the kamacite side (ABRAHAM and HORNBOGEN, 1974). However, it is more plausible that it will form in the phase with the lowest solubility for P, $i.e.$ in the taenite, as shown in the figure. The particle will pin the interface which will eventually sweep around it, as shown, leaving a nickel-rich rim, as shown. This situation will be most pronounced when the $\gamma \rightarrow \alpha$ transformation occurs at low temperatures so that Ni enrichment ahead of the interface will result from sluggish diffusion; $i.e.$ especially for ~ 7 to 8% Ni meteorites. Another condition is high P content (3 to 4%) so that phosphide precipitation occurs during transformation. The rim will contain less nickel during the early stages of transformation and more during the later stages. This will affect the thickness of the taenite structure; $i.e.$ thin early, thick later.

Another unusual structure in Allan Hills 762 is the formation of small kamacite areas within the narrow taenite bands. In essence, these are a form of plessite which formed from relatively high Ni taenite ($\sim 30\%$ Ni) during prolonged cosmic heating around 500°C. The typical broad taenite zones in high nickel meteorites contain $\sim 20\%$ Ni and considerable supercooling occurs (to ~ 400°C) before a bainitic transformation occurs forming plessite in the center of the bands. In Allan Hills 762 the taenite bands are high nickel throughout and the α phase nucleates at higher temperatures (~ 500°C) forming coarser structures. This structure should occur in other very coarse octahedrites that have cooled particularly slowly.

Allan Hills 762 is similar in composition, in structure type and genetic group to Neptune Mountain (BUCHWALD, 1975) also found in the Antarctic. It is tempting, despite their great separation, to associate them with the same meteorite shower. However, group IAB meteorites are rather abundant and the chance of finding two out of about 10 irons to date in Antarctica is quite high. However, more detailed analysis to verify or discount their common origin is worth consideration.

References

Abraham, K. and Hornbogen, E. (1974): Keimbildung metallischer Phasen in Stein-Eisen-meteoriten. Sonderdr. Z. Metallkd., **65** (11), 702–708.

Buchwald, V. F. (1975): Handbook of Iron Meteorites, Their History, Distribution, Composition and Structure. Vols. **1–3**. University of California Press.

Cassidy, W. A., Olsen, E. and Yanai, K. (1978): Antarctica; A deep-freeze store house for meteorites. Science, **198**, 727–731.

Fisher, R. M., Spangler, C. E., Jr. and Nagata, T. (1978): Metallographic properties of Yamato iron meteorite, Yamato-75031 and stony iron meteorite, Yamato-74044. Mem. Natl Inst. Polar Res., Spec. Issue, **8**, 248–259.

Goldstein, J. I. and Ogilvie, R. E. (1965): The growth of the Widmanstätten pattern in metallic meteorites. Geochim. Cosmochim. Acta, **29**, 893–920.

Goldstein, J. I. and Doan, A. S., Jr. (1972): The effect of phosphorus on the formation of the Widmanstätten pattern in iron meteorites. Geochim. Cosmochim. Acta, **66**, 51–69.

Nagata, T. (1975): Yamato Meteorites Collected in Antarctica in 1969, ed. by T. Nagata. Mem. Natl Inst. Polar Res., Spec. Issue, **5**, 110 p.

Nagata, T. (1978): A possible mechanism of concentration of meteorites within the Meteorite Ice Field in Antarctica. Mem. Natl Inst. Polar Res., Spec. Issue, **8**, 240–247.

Nagata, T., Fisher, R. M. and Sugiura, N. (1976): Metallographic and magnetic properties of a Yamato iron meteorite—Yamato-75105. Mem. Natl Inst. Polar Res., Ser. C, **10**, 1–11.

Scott, E. R. D. and Wasson, J. T. (1975): Classification and properties of iron meteorites. Rev. Geophys. Space Phys., **13**, 527–546.

Wood, J. A. (1967): Chondrites: Their metallic minerals, thermal histories, and parent planets. Icarus, **6**, 1–49.

Yanai, K. (1975): Chishitsu (Geology). Nihon Nankyoku Chiiki Kansokutai Dai-15-ji-tai Hôkoku (Report of the 15th Japanese Antarctic Research Expedition), Tokyo, National Institute of Polar Research, 72–76.

Yanai, K. (1977): First meteorites found in Victoria Land, Antarctica, December 1976 and January 1977—Report of the U.S.-Japan joint program titled "Antarctic Search for Meteorites" 1976–1977. Mem. Natl Inst. Polar Res., Spec. Issue, **8**, 51–69.